Protein Induced Aggregation of Conjugated Polyelectrolytes Probed with Fluorescence Correlation Spectroscopy: Application to Protein Identification

Danlu Wu and Kirk S. Schanze*

Department of Chemistry, University of Florida, Gainesville, Florida 32611-7200, United States

S *Supporting Information*

ABSTRACT: The interaction of a series of water-soluble conjugated polyelectrolytes with varying backbone structure, charge type (cationic and anionic), and charge density with a set of seven different proteins is explored by using fluorescence correlation spectroscopy (FCS). The FCS method affords the diffusion time for a particular CPE/protein pair, and this diffusion time is a reflection of the aggregation state of the polymer/protein in the solution. The diffusion time is larger for oppositely charged CPE/protein combinations, reflecting the tendency toward the formation of CPE/protein aggregates in these systems. However, by careful analysis of the data, other factors emerge, including possible effects of hydrophobic interaction in specific CPE/protein systems. The final diffusion time for each CPE/protein mixture varies and the diffusion time response pattern created by the six-CPE array for a typical protein is unique, and this effect was leveraged to develop a sensor array for protein identification by using linear-discriminant analysis (LDA) methods. By application of multimode linear discrimination analysis, the unknown protein samples have been successfully identified with a total accuracy of 93%.

KEYWORDS: *conjugated polyelectrolyte, fluorescence correlation spectroscopy, protein identification, protein/polymer aggregation*
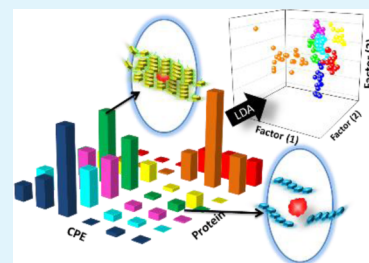
■ INTRODUCTION

Conjugated polyelectrolytes (CPEs) composed of ionic charged groups and a π-conjugated backbone are capable of water solubility and self-assembly.[1−5] Many different types of CPEs have been synthesized with various conjugated backbones, including poly(*para*-phenylene ethynylene) (*p*-PPE),[6] polythiophene,[7] and poly(*meta*-phenylene ethynylene) (*m*-PPE),[8] and various ionic groups, such as sulfonate (SO_3^-),[8,9] carboxylate (CO_2^-),[10] and quarternary ammonium (NR_3^+),[11,12] either branched[10,12] or linear.[8,9,11,13] The diversity in the polymer structures endows CPEs various hydrodynamic radii or chain conformations in aqueous solution. For example, *meta*-linked (phenylene ethynylene) chains with more than five repeat units adopt a helical structure in aqueous solution.[8,14] Most *para*-linked (phenylene ethynylene)s with linear ionic side groups spontaneously aggregate in water.[9,13,15] By contrast, specific CPEs with a high charge density, such as with branched ionic side chains, are molecularly dissolved as isolated polymer chains in water.[10,12] Thus, in general, it is possible to say that the charge and structural nature of CPE facilitates controlling the strength of interaction as well as the distance between CPE chains and other ionic species in solution.

Interaction between CPEs and proteins in aqueous solution have been the subject of considerable interest.[16−23] On the basis of studies of optical spectra, it has been inferred that the "non-specific CPE/protein" interactions cause significant change in both conformations and photophysical properties of CPEs.[16,17,19,21] For example, Bazan and co-workers found that an anionic sulfonated poly(*para*-phenylenevinylene)

(PPV), mixed with small amounts of various proteins, including positively charged avidin and tau, as well as negatively charged bovine serum albumin (BSA) and pepsin A individually, resulted in several-fold increase in fluorescence intensity from the polymer. These effects are attributed to interactions between the anionic PPV and the proteins via electrostatic and hydrophobic forces.[16] Bunz and co-workers also reported that BSA could enhance the fluorescence of carboxylate-substituted CPEs, while a series of proteins, such as histone, lysozyme, myoglobin, and hemoglobin quenched the fluorescence of CPEs due to the formation of a complex.[21] Meanwhile, some sensing assays have been developed for protein recognition by employing fluorescence intensity change pattern of CPEs.[19,21,24]

In the present study, we explore the aggregation state change of CPEs induced by interaction with various proteins by focusing on the diffusion dynamics of the resulting CPE/protein aggregates. In previous work, it has been shown that the conformation state and size change of fluorescent macromolecules can be monitored by fluorescence correlation spectroscopy (FCS).[18,25−28] FCS is based on analysis of the fluorescence fluctuation signals from fluorescent particles in a confocal sample volume.[29] The technique provides insight regarding diffusion behavior of the molecules at the single molecule (or particle) level in solution, which is closely related

to the molecular weight, size and conformation of fluorescent species. Accordingly, the diffusion behavior change reflects the chemical or physical change in the fluorophores as well as the surrounding environments.[30,31] FCS has previously been employed to study the conformation change of many large molecules. Specifically, Borsch and co-workers used FCS to monitor protein folding and unfolding transitions.[27] Schwille and co-workers conducted research on the fluorescence fluctuations of green fluorescence protein (GFP) by FCS and revealed the relationship between structural changes of GFP and its fluctuations in emission, making it possible to probe the local pH.[25] Waldeck and co-workers used FCS to uncover the three regimes in the hydrodynamic radius for complexes formed from an anionic CPE and a surfactant in aqueous solution.[18] In recent work, we have applied FCS to investigate the structure and aggregation of a dye-ligand intercalation complex formed between a helical CPE, a biotin-chromophore complex and avidin.[32] This previous work demonstrates that FCS is a promising tool for monitoring the aggregation state and size change of fluorescent conjugated polyelectrolytes as they interact with biopolymers in solution.

The current study explores how the aggregation state or size of six CPEs change when they are exposed to solutions of seven different types of proteins, which is accomplished by measuring their diffusion time through FCS and analyzing their diffusion behavior change. If the charges of the CPEs and proteins are opposite, the electrostatic attraction induced aggregation can cause the increase in diffusion time of CPEs; by contrast, if the CPE and protein have the same charge type, deaggregation will occur for CPEs apparently due to repulsive interaction between two macromolecules, resulting in a decrease in diffusion time. Meanwhile, other factors including hydrophobic interaction, charge density, molecular weight, and polymer backbone structure also influence the final sizes and conformations of CPEs. As a result, the final diffusion time for each CPE-protein mixture varies and the diffusion time response pattern created by the six-CPE array for a typical protein is unique, which can be utilized for protein recognition and distinction.

By taking advantage of this unique interaction pattern, a sensor array comprising six CPE probes with various charge properties, structure characteristics and molecular structure is developed for seven proteins, which also have various isoelectric points (pI), molecular weights, and structures. Each type of protein can be classified via linear discriminant analysis (LDA) of the FCS signal responses. The combination of sensor array with LDA has been applied in many sensing strategies.[19,33−35] In the current paper, multiple LDA operations are employed for training the FCS-based data matrix and creating a series of discriminant spaces/plots for classifying different proteins. Then, the technique readily identifies a series of unknown protein samples with recognition accuracy ~93%. Unlike the conventional sensors requiring specific label or marker design and synthesis, the CPE probes do not require covalent attachment to a target but undergo self-assembly via nonspecific interaction. This novel protein sensor array will make contribution to the medical diagnostics or clinical research,[36−39] where the detection of more than one protein in one single technical setting is highly preferred.

■ EXPERIMENTAL SECTION

Materials. Avidin from egg white (avidin, A9275), lysozyme from chicken egg white (LYZ, L6876), peroxidase from horseradish, type I (HRP, P8125), phospholipase D from *Arachis hypogaea* (peanut), type

II (PLD2, P0515), hexokinase from *Saccharomyces cerevisiae*, type III (HK3, H5000), albumin from bovine serum (BSA, A2153), glucose oxidase from *Aspergillus niger* (GOx, G7141), Coomassie brilliant blue G-250, phosphoric acid, and methanol (HPLC grade) were purchased from Sigma-Aldrich. The synthesis procedures and characterization of **P1**,[40] **P2**,[8] **P3**,[9] **P4**,[13] **P5**,[11] and **P6**[13] have been previously reported. All sample solutions were prepared using water that was distilled and purified by a Millipore purification system (Millipore Simplicity ultrapure water system). Buffer solutions were prepared with reagent-grade materials (Fisher). All concentrations of polymers are provided in polymer repeat unit concentration (PRU). Concentrated stock solutions of the CPEs and proteins were prepared separately in buffer to obtain the desired concentrations. Each single CPE/protein pair was mixed well before FCS measurement. The unknown protein/CPE samples were prepared in the same manner as the known samples, but they were prepared by an assistant so that the sample identity was unknown during the analysis. All assays were conducted in 5 mM phosphate buffer, pH 7.2 at room temperature. The Bradford protein assay was conducted according to a literature procedure.[41]

Instrumentation. The measurements were performed on an FCS setup constructed in house. The FCS system was developed by using an Olympus IX70 epi-fluorescence microscope platform. A 405 nm diode laser (Coherent, CUBE) was employed as the excitation light source. After passing a spatial filter, a 405 nm single mode fiber, and a fiberport collimator, the laser beam was expanded and collimated to 4.4 mm in diameter. The beam was then focused onto the sample though an objective lens (Olympus, 60×, numerical aperture 1.2, water immersion), forming a femtoliter confocal volume. The fluorescence was collected by the same objective, separated from the excitation light by a dichroic mirror (Chroma, 405 nm), then split by a 50/50 cube splitter and directed into an avalanche photodiode (APD, PerkinElmer, SPCM-AQR-14-FC) through a 50 μm-inner diameter optical fiber after passing through a 500 ± 20 nm bandpass filter. Chambered coverglass (Thermo Scientific, Nunc, Lab-Tek) was used as the sample container. In each FCS experiment the fluorescence fluctuations were measured for 1−2 min. Free fluorescein ($D = 3.00 \times 10^{-10}$ m²·s⁻¹)[42] was used for calibration. Autocorrelation was processed by a hardware correlator (correlator.com, Flex02-12D).

UV−visible absorption spectra were measured in 1 cm light path disposable polystyrene cuvettes or 1 mm light path quartz cuvettes on a UV−vis spectrophotometer (Shimadzu, UV-1800).

Theory of Fluorescence Correlation Spectroscopy. FCS focuses on the emission fluctuations from the fluorophores that are diffusing through the excitation volume, which are characterized by an autocorrelation function, $G(\tau)$:[30]

$$G(\tau) = \frac{\langle F(t) \cdot F(t+\tau) - F(t) \rangle^2}{\langle F(t) \rangle^2} = \frac{\langle \delta F(t) \cdot \delta F(t+\tau) \rangle}{\langle F(t) \rangle^2} \quad (1)$$

where $\delta F(t)$ represents the fluctuation of the fluorescence signal $F(t)$ at time t. An explicit expression for $G(\tau)$, representing a single-component solution in a three-dimensional (3D) space, is used for data analysis.[31,43−45]

$$G_{3D}(\tau) = \frac{1}{N} \frac{1}{1 + \frac{\tau}{\tau_D}} \frac{1}{\sqrt{1 + \frac{\tau}{\omega^2 \tau_D}}} \quad (2)$$

In this expression ω is the structure parameter, which equates to (ω_z/ω_r), where ω_z is the longitudinal radius and ω_r is the transversal or waist radius of the confocal volume, N is the average number of fluorescent molecules in the detection volume, and τ_D is the average time spent by a fluorescent molecule in the detection volume.

■ RESULTS AND DISCUSSION

Fluorescence Correlation Spectroscopy Diffusion Times of CPE/Protein Complexes. A set of six CPEs consisting of three with anionic and three with cationic side chains were chosen for exploring their interactions with proteins. The CPE structures with their abbreviations are

7644

dx.doi.org/10.1021/am5009437 | *ACS Appl. Mater. Interfaces* 2014, 6, 7643−7651

Scheme 1. Chemical Structures of Six Conjugated Polyelectrolytes
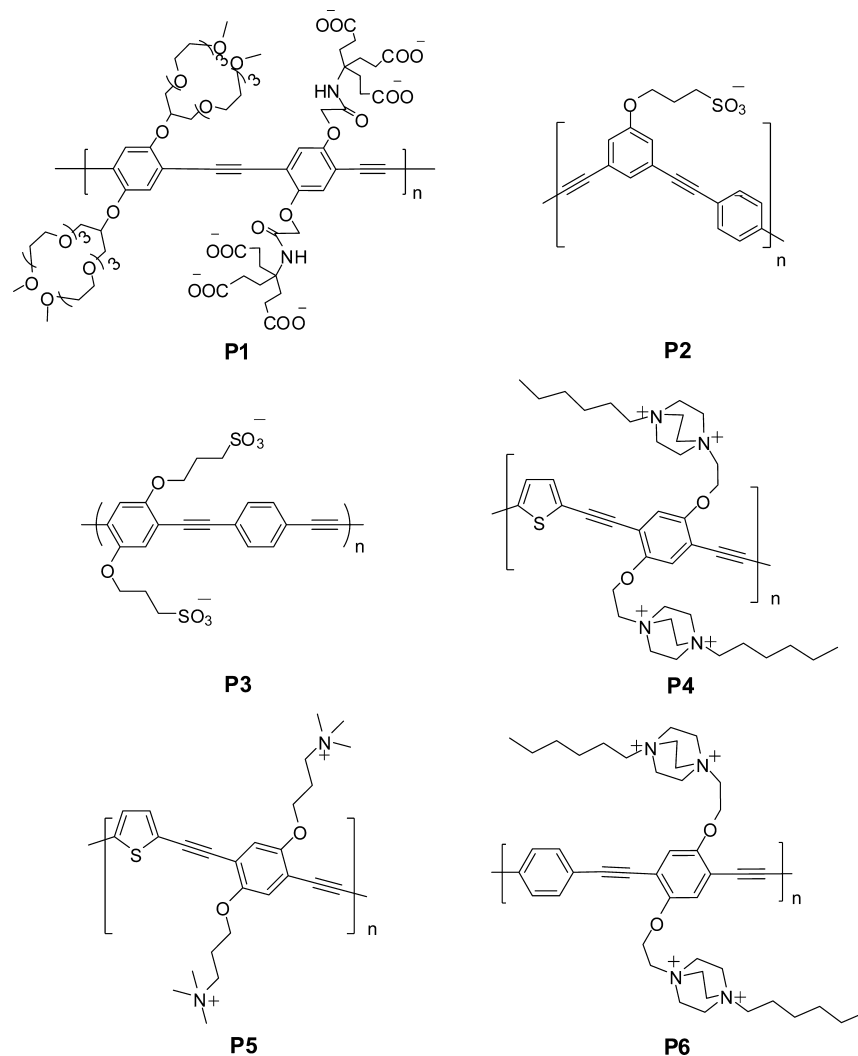
Table 1. Properties of Conjugated Polyelectrolytes

	P1	P2	P3	P4	P5	P6
estimated MW (kDa)	11.0	~40.0	~100.0	7–70	n/a	7–70
τ_d (10^{-5} s)^a	8.4 ± 0.9	29.4 ± 3.0	101.3 ± 25.9	21.7 ± 3.9	27.3 ± 3.1	24.0 ± 8.6
charge on PRU	6(−)	1(−)	2(−)	4(+)	2(+)	4(+)

^{a}Diffusion times (τ_d) measured in 5 mM HEPEs buffer, pH 7.2, room temperature by FCS.

shown in Scheme 1, and their estimated molecular weights are listed in Table 1. Among those CPEs, **P1** is not aggregated in aqueous solution due to its bulky and highly charged side chains that prevent hydrophobic interchain interactions by increasing the electrostatic repulsion between polymer chains. The other five CPEs are aggregated to various extents in water due to the hydrophobic effect and π−π stacking interactions. The cationic CPEs **P4** and **P6** are less aggregated than **P3** due to their relatively long cationic bisalkylammonium side groups that provide a steric barrier between the π-conjugated chains.[13] Anionic CPE **P2** with *meta*-linked backbone self-assembles into a helical conformation in aqueous solution, and its helix can serve as a host for small molecule intercalators.[8,14,32,46] Although it is not possible to apply gel permeation chromatography to measure the absolute molecular weights (MW) for **P2-P6** due to their amphiphilic nature, other

techniques have been used to estimate their MWs,[8,9,13] and the results are displayed in Table 1. Due to their various molecular weights and conformations, this set of six CPEs displays different diffusion behavior as reflected by the FCS diffusion time summarized in the bottom row of Table 1. It is seen that CPEs with higher molecular weight generally display longer diffusion times

Seven proteins were used in this work and their properties are summarized in Table 2 along with the acronyms that are used herein. Avidin and LYZ have isoelectric point (pI) > 7, exhibiting positive charge in neutral solution; PLD2, HK3,[47] BSA, and GOx have pI < 7, so they are negatively charged in neutral solution. However, for the protein HRP, due to its complexity, it is difficult to determine its pI value.[48] Those proteins also feature different molecular weights varying from 14 to 200 kDa and distinct structural characteristics.

Table 2. Properties of Proteins

abbreviation	protein	MW (kDa)	pI
avidin	avidin	66	10
LYZ	lysozyme	14	11.0
HRP	horseradish peroxidase, type I	44	3−9
PLD2	phospholipase d, type II	200	4.65
HK3	hexokinase type III	54	PI:5.25 PII: 4
BSA	bovine serum albumin	66	4.7
GOx	glucose oxidase	160	4.2

To quantitatively test the interaction between the CPEs and proteins, all the experimental conditions including concentrations of both CPEs and proteins, ionic strength, and pH of buffer solution (pH = 7.2) are fixed. The concentrations of proteins are determined through Bradford protein assay, a dye-binding assay in which the color change of dyes occurs in response to various weight concentrations of protein.[49] Each of the six CPEs is mixed with the seven proteins individually in 5 mM HEPEs buffer with final [CPE] = 500 nM (in repeat units) and [protein] = 2 μg/mL (this concentration was carefully selected so that the signal-to-noise ratio was adequate and the signal was within the linear range of the detector). Twenty replicates are prepared for each CPE-protein pair and all the samples are submitted for FCS measurement in sequence.

Figure 1 illustrates a typical FCS measurement result for the cationic CPE, **P4**, with and without proteins. (Note that the
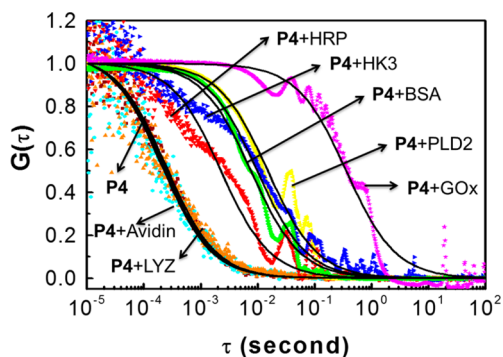

Figure 1. Normalized FCS correlation function curves for **P4** without protein (■) and with Avidin (●), LYZ (▲), HRP (▼), HK3 (▶), BSA (◆), PLD2 (◀), and GOx (★) in 5 mM HEPEs buffer pH 7.2. Black solid lines are the single species fitting curves.

peaks that appeared on the curves, τ = 0.01−2 s, were artifacts in the FCS system.[50,51]) Based on the FCS curves, the mixtures of **P4** with avidin (τ_d = 20.7 × 10^{-5} s) or LYZ (τ_d = 22.5 × 10^{-5} s), whose pI value >10, have approximately the same diffusion times as pure **P4** (τ_d = 21.7 × 10^{-5} s). By contrast, the other five proteins, whose pI average < 7, to various degrees, induce the aggregation of **P4** and a dramatic increase in the diffusion times is observed. The order for the diffusion rate of **P4**/ proteins is HRP > BSA > HK3 > PLD2 > GOx with increasing τ_d = 1.95, 5.66, 7.80, 13.0, and 219.00 ms, respectively. Due to the polydisperse nature of the aggregates, the FCS curves are a combination of several single-species curves with different diffusion times. Nevertheless, the fitting eq 2 is still applied and an average diffusion time for each CPE/protein aggregate is thereby obtained. As stated above, HRP and HK3 are the mixtures of several isozymes, whose FCS curves are more complicated and therefore are difficult to fit by the single
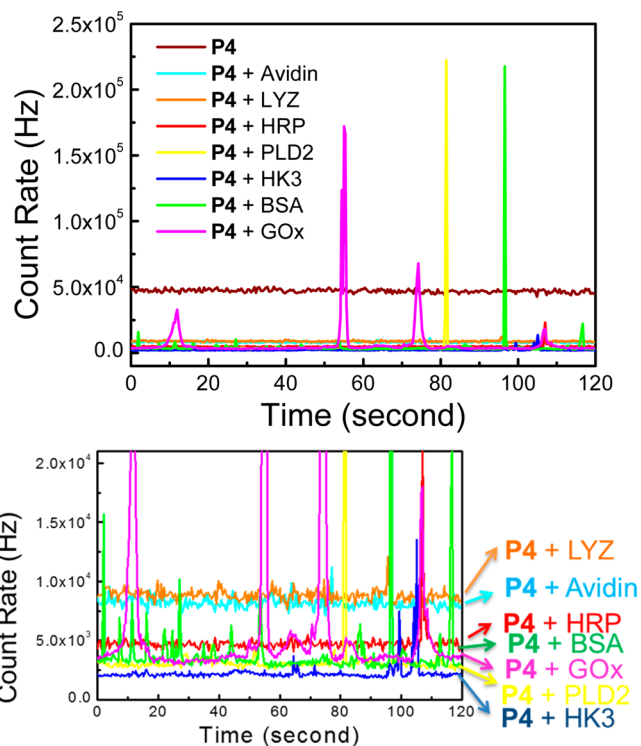

Figure 2. Top: Fluorescence intensity fluctuation profile for **P4** without and with seven proteins. Bottom: enlargement of the fluctuation profile for **P4** with seven proteins. ([**P4**] = 500 nM, [protein] = 2 μg/mL in 5 mM HEPEs buffer pH 7.2)

species fitting equation. The fluorescence fluctuation profiles for each mixture are displayed in Figure 2. The more intense and broader peaks correspond to the larger aggregates passing through the excitation volume which lead to longer diffusion times as shown in Figure 1. Those time-dependent profiles also provide the evidence for heterogeneity or size multidistribution of aggregated CPEs.

The FCS results for all of the samples are shown as a bar graph in Figure 3 in terms of log (τ_d/τ_0), where τ_d and τ_0 are
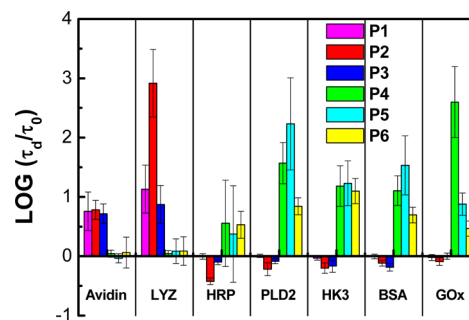

Figure 3. Log (τ_d/τ_0) response 2-dimensional bar plot of six CPEs mixed individually with seven proteins. Bar height is the average value of 20 replicates for each CPE/protein pair.

the diffusion times of CPE with and without protein, respectively. The error bars represent the calculated standard deviation for 20 individual diffusion time replicate measurements for each sample. Figure 4 is the 3D column graph for the FCS results. The row with the same color corresponds to a given protein and the charge type for each species is embodied
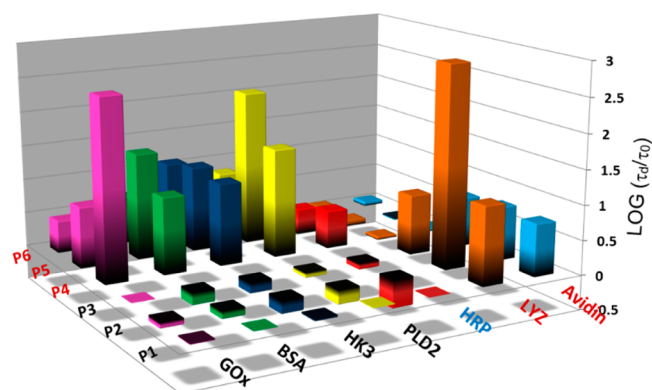
Figure 4. Log (τ_d/τ_0) response 3-dimensional column pattern of six CPEs mixed individually with seven proteins. Column height is the average value of 20 replicates for each mixture. In this presentation some of the columns correspond to negative values, that is, $\log(\tau_d/\tau_0) < 0$. In order to make the negative values clear, the columns are shaded dark for $\log(\tau_d/\tau_0) \sim 0$. Therefore, for columns with dark color at the bottom $\log(\tau_d/\tau_0) > 0$, and for columns with dark color at the top $\log(\tau_d/\tau_0) < 0$.

in their abbreviations by color: negative charge is black, positive charge is red, and the protein HRP with mixed pI is blue.

There are several clear trends that emerge upon inspection of the data in Figures 3 and 4. First, it is clear that the diffusion

time increases (i.e., log $(\tau_d/\tau_0) > 0$) for the oppositely charged CPE/protein pairs, such as LYZ/**P1** or PLD2/**P4**, due to the electrostatic attraction induced formation of polymer/protein aggregates. In sharp contrast, when the charge of the protein and CPE are the same, especially for the pairs of anionic CPEs and proteins with pI < 7 such as PLD2/**P2** or HK3/**P3**, the mixtures exhibit shorter diffusion time compared to the CPE alone (i.e., log $(\tau_d/\tau_0) < 0$). Apparently the Coulombic repulsion between the two negatively charged macromolecules disrupts the aggregation of CPEs. For the cationic CPEs with positively charged proteins, such as LYZ/**P5** or **P6**, some aggregation appears with the average log (τ_d/τ_0) varying in the range 0−0.1. This is likely due to a hydrophobic interaction between the CPE chains and the protein.[20]

Note that the much larger error bars observed for HRP/CPE pairs (e.g., HRP/**P5**) is presumably due to the complexity in the mixture of protein isozymes with various pI values, which greatly single HRP out from other proteins. Based on the average log (τ_d/τ_0) values for HRP with various CPEs, HRP is able to induce aggregation when mixed with cationic CPEs, while disrupting aggregation when mixed with anionic aggregated CPEs. Therefore, HRP displays anionic characteristics in neutral pH.

Besides electrostatic or hydrophobic interaction, other factors may also influence the final response. For example, the log (τ_d/τ_0) for anionic **P2** with cationic LYZ (pI = 11) is much larger

Scheme 2. Training Results for Multiple LDA Operation of Diffusion Time Response for Six CPE Probes against Seven Proteins[a]

1st LDA training

	Avidin	LYZ	HRP	PLD2	HK3	BSA	GOx	Sum
Error/total	0/20	0/20	4/20	7/20	7/20	5/20	1/20	24/140
Training Accuracy	100%	100%	80%	65%	65%	75%	95%	83%

2nd LDA training

	Avidin	LYZ	HRP	PLD2	HK3	BSA	GOx	Sum
Error/total	0/20	0/20	2/20	2/20	2/20	1/20	1/20	8/140
Training Accuracy	100%	100%	90%	90%	90%	95%	95%	94%

3rd LDA training

	Avidin	LYZ	HRP	PLD2	HK3	BSA	GOx	Sum
Error/total	0/20	0/20	2/20	2/20	0/20	1/20	1/20	6/140
Training Accuracy	100%	100%	90%	90%	100%	95%	95%	96%

4th LDA training

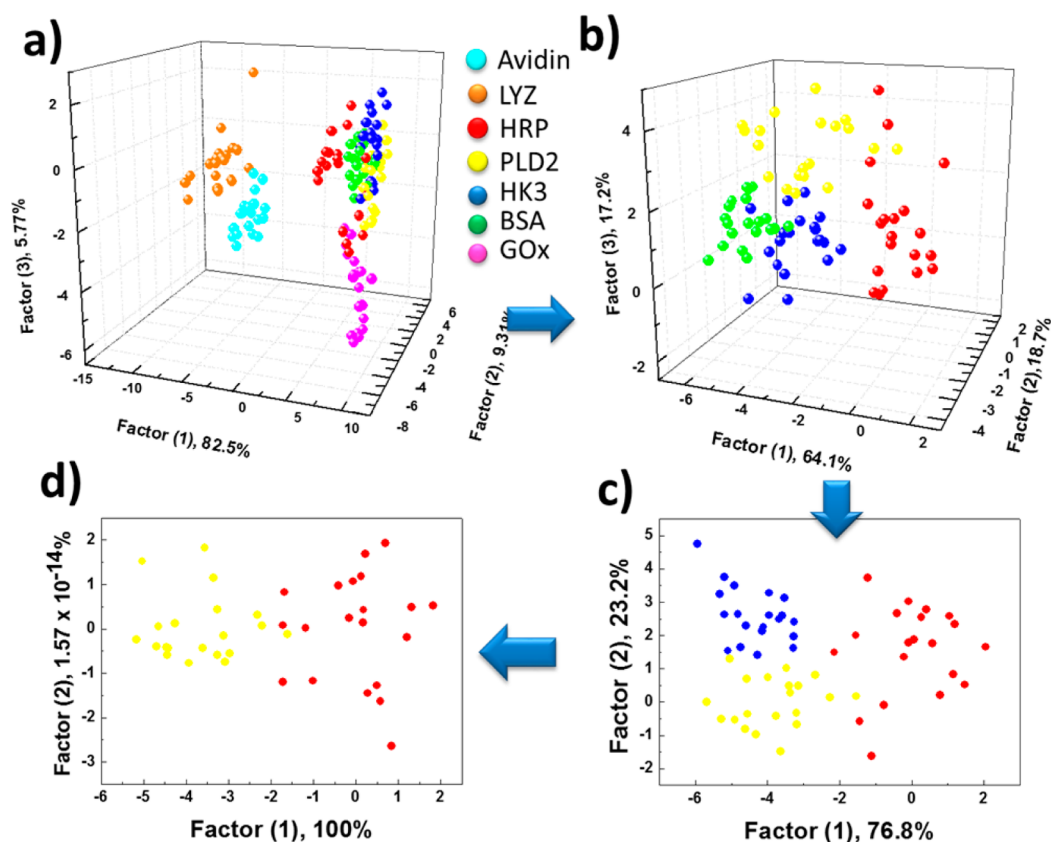|	Avidin	LYZ	HRP	PLD2	HK3	BSA	GOx	Sum
Error/total	0/20	0/20	0/20	1/20	0/20	1/20	1/20	3/140
Training Accuracy	100%	100%	100%	95%	100%	95%	95%	98%

[a]20 replicates for each probe-target pair.

Figure 5. Linear discriminant analysis factor spaces for the diffusion time response patterns obtained with six CPE probes sensor array against (a) seven proteins (avidin, LYZ, HRP, PLD2, HK3, BSA, GOx), (b) four proteins (HRP, PLD2, HK3, BSA), (c) three proteins (HRP, PLD2, HK3), (d) two proteins (HRP, PLD2). Twenty replicates for each CPE-protein pair.

compared to that of **P2** with avidin (pI = 10). We attribute this phenomenon to the high charge density of LYZ, which has the smallest molecular weight (44 kDa) but highest pI value. However, when considered the cationic **P4** with a series of anionic proteins, the molecular weight of the protein seems to have an impact on the final diffusion time change. The value of log (τ_d/τ_0) for **P4**/proteins increases roughly as the increase of the molecular weight of the protein: HRP (44 kDa) < HK3 (54 kDa) ≈ BSA (66 kDa) < PLD2 (200 kDa) < GOx (160 kDa). However, this trend does not apply to other types of oppositely charged CPE/protein mixtures.

In addition to the influence of the protein, the properties of the polymers also affect the diffusion time of the CPE/protein mixtures. For example, the thiophene containing CPEs (**P4** and **P5**) appear to form larger aggregates compared to the **P6**, which contains only phenylene repeat units. In particular, when **P4** is mixed with oppositely charged proteins (BSA, HK3, PLD, GOx), the resulting log (τ_d/τ_0) values are larger than those for **P6** with the same proteins. This finding is consistent with the previous reports that the thiophene containing CPEs appear to have a larger hydrophobic character compared to the phenylene analogues.[52] The molecular structure and conformation of the polymer backbone may also influence the interaction between CPEs and proteins. For instance, the diffusion time for **P2**, a helical CPE, mixed with oppositely charged proteins (LYZ, avidin), is greater than that of **P3**, which has a linear backbone, even though **P3** has a higher MW than **P2** does. Consequently, the final signal response is affected by many elements including charge type, charge density, molecular weight, and structure property of both proteins and CPEs. It is difficult to
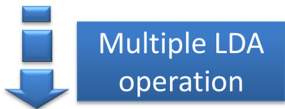
deconvolute each part just relying on the FCS measurements. We are pleased to find that the six CPEs display a unique signal response pattern for each protein, which is beneficial for identification of proteins as shown in the next section.

Protein Sensing: Linear Discriminant Analysis of FCS Diffusion Times for Protein/CPE Mixtures. In order to provide more insight into the structure−property relationships for the CPE/protein mixtures, we carried out studies aimed at subjecting the FCS results to linear discriminant analysis (LDA, the details of the theory and procedures for LDA can be found in the literature).[53,54] As outlined below, this work led to the development of a novel CPE-FCS based method allowing the identification of a protein in an unknown sample. As can be seen below, a single LDA operation on the entire set of data was unable to afford a high degree of accuracy due to the fact that a single LDA was originally developed for two-class problems and it is suboptimal if multiple classes are considered.[55] Thus, we applied a sequence of LDA steps afterward to multiple subgroups of proteins and generated subspaces that have higher overall classification power.[56]

The details about the multiple LDA process can be found in Scheme 2. Initially, we used the full set of log (τ_d/τ_0) values to construct a matrix consisting of 6 CPEs × 7 proteins × 20 replicates for LDA analysis (Supporting Information Table S1). The eigenvectors that maximize the ratio of between-class variance to the within-class variance are obtained through LDA implemented as a script in Matlab. Then the three most significant eigenvectors (carrying 82.5, 9.31, and 5.77% of the discriminant information, respectively, Supporting Information Table S3) are used to plot sample data in a 3D discriminant

7648

dx.doi.org/10.1021/am5009437 | ACS Appl. Mater. Interfaces 2014, 6, 7643−7651

Scheme 3. Test Results for Multiple LDA Operation of Diffusion Time Response for Six CPE Probes against Forty-Two Unknown Protein Samples

	Avidin	LYZ	HRP	PLD2	HK3	BSA	GOx	Sum
Error/total	0/6	0/6	1/6	0/6	1/6	3/6	0/6	5/42
Test Accuracy	100%	100%	83%	100%	83%	50%	100%	88%

Multiple LDA operation

	Avidin	LYZ	HRP	PLD2	HK3	BSA	GOx	Sum
Error/total	0/6	0/6	1/6	0/6	0/6	2/6	0/6	3/42
Test Accuracy	100%	100%	83%	100%	100%	66.7%	100%	93%

space as shown in Figure 5a. The $6 \times 7 \times 20$ samples are presented with different colors denoting the different proteins. In principle, each protein should occupy a specific region in the 3D space and the different proteins should be well separated from each other. As displayed in Figure 5a and Scheme 2, three protein groups of avidin, BSA, and GOx are well classified with individual accuracy ≥95%. However, mingling occurs among the categories of HRP, PLD2, HK3, and BSA with error to be 4/20, 7/20, 7/20, and 5/20, respectively, resulting in the total classification accuracy 83%. A second LDA operation is applied using only the subsets of data that belong to HRP, PLD2, HK3, and BSA. A new discriminant space specifically for these four proteins is created and the improvement in the separation of groups can be easily observed (Figure 5b). The errors are reduced to be 2/20, 2/20, 2/20, and 1/20 for HRP, PLD2, HK3, and BSA, respectively, with an increased total accuracy of 94% for seven proteins (Scheme 2). More LDA operations are continuously applied for those groups with relatively lower individual training accuracy (<95%). As shown in Figure 5c, d and Scheme 2, after four LDA operations, the total classification accuracy for the entire seven proteins is 98%, much higher than the result of a single LDA operation, that is, 83%. By utilizing multiple subspaces instead of a single large space, the protein discriminant method is well established (four sets of eigenvalues are summarized in Supporting Information Table S3). We note that this discrimination method is typically designed for the experimental conditions in which [protein] = 2 μg/mL. A series of similar measurements for [protein] = 1 μg/mL and 5 μg/mL were also conducted and different discrimination patterns were obtained for each concentration (data not shown). However, the lower concentration ([protein] = 1 μg/mL) led to lower signal-to-noise ratio, while high concentration ([protein] = 5 μg/mL) resulted in a very high signal (which could exceed the detector linear response region). Consequently, these two target concentrations were not selected for our protein sensing application. Nevertheless, the limit of detection for our sensing array is equal to or below 1 μg/mL.

Succeeding in classifying known samples, we next focus on detection and identification of unknown protein samples (Supporting Information Table S2). Forty-two artificial protein samples prepared by a second researcher were subjected to the same protocol as described above, including determining concentration through Bradford protein assay, mixing proteins

with 6 CPE probes individually, adjusting concentration to [CPE] = 500 nM and [protein] = 2 μg/mL, conducting FCS measurements and generating the final data matrix.

As processed by first level LDA operation, the entire unknown samples are projected to the discriminant space built up in the above training process. As followed the theory of LDA,[53,54] in the created 3D discriminant space, the Mahalanobis distances of each unknown spot in the space to the centroid of each class are calculated and these unknown spots are assigned and identified according to the shortest Mahalonobis distance. Based on the classification accuracy obtained in the training process, the samples that were assigned to the groups of avidin, LYZ, and GOx are believed to be identified with accuracy >95%. The subset data belonging to those three proteins are removed from the entire matrix, and the rest of the matrix is resubmitted for a second level LDA operation and processed in a similar manner. By using this sequence of four LDA operations, all of the unknown samples are identified. The verification is assisted by the researcher who prepares unknown samples, and the resulting error report is shown in Scheme 3. Total identification accuracy is improved from 88% (failure test: 1 for HRP, 1 for HK3, and 3 for BSA) for a single LDA operation to 93% (failure test: 1 for HRP and 2 for BSA) for a multiple LDA operation (final failure test samples are marked with stars in Supporting Information Table S2).

Based on the LDA results discussed above, we find that proteins with pI > 7, such as avidin and LYZ, are easily separated from the rest of the group of proteins with classification/identification accuracy ~100% for both known and unknown samples, followed by GOx (pI = 4.2) with classification/identification accuracy 95% and 100% for known and unknown samples, respectively. HRP, PLD2, HK3, and BSA are harder to distinguish, likely due to their similarity in charge properties, resulting in similar interaction with each CPE and requiring further LDA processing to allow their resolution. The complexity in the pI value for multi-isozyme mixture, such as HRP, makes the data the most spread out in the discriminant spaces, which introduces more difficulty in their classification and identification. Nevertheless, after applying multiple LDA, those proteins are still can be classified and identified with relatively high accuracy.

Based on the discussion above, the separation of proteins with opposite charge type is the easiest to accomplish,

suggesting the charge type plays the most significant role in the interaction between CPEs and proteins as well as the recognition of proteins. While further discriminant between proteins with similar charge properties needs more analysis on the minor differences in data matrix. Those differences probably arise from hydrophobic interaction, molecular structure, charge density or molecular weight of both CPEs and proteins. As discussed above, those factors can also make their own contributions to the differentiation of proteins.

CONCLUSION

In sum, we have conducted a systematic investigation on the aggregation state/size change of CPEs induced by nonspecific interaction between various CPEs and proteins from single particle diffusion times as measured by fluorescence correlation spectroscopy. Many factors including charge type, charge density, hydrophobic interaction, molecular weight and structure of CPEs or proteins play a role in determining the final diffusion behaviors of CPEs, among which, charge type plays the essential role. The patterns of log (τ_d/τ_0) signal responses generated by six CPEs are distinct for different proteins, giving rise to a novel CPE based sensor array for proteins. By applying multivariate pattern recognition chemometrics, LDA, in a multiple operation mode, a series of discriminant spaces is created and seven different proteins have been successfully classified. Then forty-two unknown samples are further tested and a relatively high identification accuracy 93% is obtained, which verifies the robustness and feasibility of this novel sensor array. This type of sensing strategy establishes a new protein sensing platform where the proficient manipulation and strong biological background are not required for operators. Further effect can be made upon the optimization of probes including improving the purity of the polymer samples, conjugating more versatile functional groups to the backbone or introducing new CPE probes. Moreover, the development of the sensor array in more complicated biological environments is necessary to eliminate potential interference and enhance their feasibility in real world applications.

ASSOCIATED CONTENT

Ⓢ Supporting Information

Original sample training data matrix, unknown sample data matrix, and eigenvalues with percentage for 4 times LDA operation. This material is available free of charge via the Internet at http://pubs.acs.org.

AUTHOR INFORMATION

Corresponding Author

*Tel.: 352-392-9133. Email: kschanze@chem.ufl.edu.

Notes

The authors declare no competing financial interest.

ACKNOWLEDGMENTS

REFERENCES

(1) Pinto, M. R.; Schanze, K. S. Conjugated Polyelectrolytes: Synthesis and Applications. *Synthesis* **2002**, 1293−1309.

(2) Thomas, S. W.; Joly, G. D.; Swager, T. M. Chemical Sensors Based on Amplifying Fluorescent Conjugated Polymers. *Chem. Rev.* **2007**, *107*, 1339−1386.

(3) Jiang, H.; Taranekar, P.; Reynolds, J. R.; Schanze, K. S. Conjugated Polyelectrolytes: Synthesis, Photophysics, and Applications. *Angew. Chem., Int. Ed.* **2009**, *48*, 4300−4316.

(4) *Conjugated Polyelectrolytes: Fundamentals and Applications*; Liu, B.; Bazan, G. C., Eds.; Wiley-VCH Verlag GmbH & Co: Weinheim, Germany, 2013.

(5) Parthasarathy, A.; Zhu, X.; Schanze, K. S. In *Conjugated Polymers: A Practical Guide to Synthesis*; Mullen, K., Reynolds, J. R., Masuda, T., Eds.; Royal Society of Chemistry: Cambridge, UK, 2014; pp 343−358.

(6) Bunz, U. H. F. Poly(aryleneethynylene)s: Syntheses, Properties, Structures, and Applications. *Chem. Rev.* **2000**, *100*, 1605−1644.

(7) Perepichka, I. F.; Perepichka, D. F.; Meng, H.; Wudl, F. Light-Emitting Polythiophenes. *Adv. Mater.* **2005**, *17*, 2281−2305.

(8) Tan, C. Y.; Pinto, M. R.; Kose, M. E.; Ghiviriga, I.; Schanze, K. S. Solvent-Induced Self-Assembly of a Meta-Linked Conjugated Polyelectrolyte. Helix Formation, Guest Intercalation, and Amplified Quenching. *Adv. Mater.* **2004**, *16*, 1208−1212.

(9) Tan, C. Y.; Pinto, M. R.; Schanze, K. S. Photophysics, Aggregation, and Amplified Quenching of a Water-Soluble Poly-(Phenylene Ethynylene). *Chem. Commun.* **2002**, 446−447.

(10) Lee, S. H.; Komurlu, S.; Zhao, X. Y.; Jiang, H.; Moriena, G.; Kleiman, V. D.; Schanze, K. S. Water-Soluble Conjugated Polyelectrolytes with Branched Polyionic Side Chains. *Macromolecules* **2011**, *44*, 4742−4751.

(11) Chemburu, S.; Ji, E.; Casana, Y.; Wu, Y.; Buranda, T.; Schanze, K. S.; Lopez, G. P.; Whitten, D. G. Conjugated Polyelectrolyte Supported Bead Based Assays for Phospholipase a(2) Activity. *J. Phys. Chem. B* **2008**, *112*, 14492−14499.

(12) Zhao, X. Y.; Schanze, K. S. Fluorescent Ratiometric Sensing of Pyrophosphate via Induced Aggregation of a Conjugated Polyelectrolyte. *Chem. Commun.* **2010**, *46*, 6075−6077.

(13) Zhao, X. Y.; Pinto, M. R.; Hardison, L. M.; Mwaura, J.; Muller, J.; Jiang, H.; Witker, D.; Kleiman, V. D.; Reynolds, J. R.; Schanze, K. S. Variable Band Gap Poly(arylene ethynylene) Conjugated Polyelectrolytes. *Macromolecules* **2006**, *39*, 6355−6366.

(14) Ji, E. K.; Wu, D. L.; Schanze, K. S. Intercalation-FRET Biosensor with a Helical Conjugated Polyelectrolyte. *Langmuir* **2010**, *26*, 14427−14429.

(15) Zhao, X. Y.; Jiang, H.; Schanze, K. S. Polymer Chain Length Dependence of Amplified Fluorescence Quenching in Conjugated Polyelectrolytes. *Macromolecules* **2008**, *41*, 3422−3428.

(16) Dwight, S. J.; Gaylord, B. S.; Hong, J. W.; Bazan, G. C. Perturbation of Fluorescence by Nonspecific Interactions between Anionic Poly(phenylenevinylene)s and Proteins: Implications for Biosensors. *J. Am. Chem. Soc.* **2004**, *126*, 16850−16859.

(17) Eftink, M. R.; Ghiron, C. A. Fluorescence Quenching Studies with Proteins. *Anal. Biochem.* **1981**, *114*, 199−227.

(18) Yue, H. J.; Wu, M. Y.; Xue, C. H.; Velayudham, S.; Liu, H. Y.; Waldeck, D. H. Evolution in the Supramolecular Complexes between Poly(phenylene ethynylene)-Based Polyelectrolytes and Octadecyltrimethylammonium Bromide as Revealed by Fluorescence Correlation Spectroscopy. *J. Phys. Chem. B* **2008**, *112*, 8218−8226.

(19) Miranda, O. R.; You, C. C.; Phillips, R.; Kim, I. B.; Ghosh, P. S.; Bunz, U. H. F.; Rotello, V. M. Array-Based Sensing of Proteins Using Conjugated Polymers. *J. Am. Chem. Soc.* **2007**, *129*, 9856−9857.

(20) Wang, D. L.; Gong, X.; Heeger, P. S.; Rininsland, F.; Bazan, G. C.; Heeger, A. J. Biosensors from Conjugated Polyelectrolyte Complexes. *Proc. Natl. Acad. Sci. U.S.A.* **2002**, *99*, 49−53.

(21) Kim, I. B.; Dunkhorst, A.; Bunz, U. H. F. Nonspecific Interactions of a Carboxylate-Substituted Ppe with Proteins. A Cautionary Tale for Biosensor Applications. *Langmuir* **2005**, *21*, 7985−7989.

7650

dx.doi.org/10.1021/am5009437 | *ACS Appl. Mater. Interfaces* 2014, 6, 7643−7651

(22) Huang, F.; Wang, X. H.; Wang, D. L.; Yang, W.; Cao, Y. Synthesis and Properties of a Novel Water-Soluble Anionic Polyfluorenes for Highly Sensitive Biosensors. *Polymer* **2005**, *46*, 12010−12015.

(23) An, L. L.; Wang, S.; Zhu, D. B. Conjugated Polyelectrolytes for Protein Assays and for the Manipulation of the Catalytic Activity of Enzymes. *Chem-Asian J.* **2008**, *3*, 1601−1606.

(24) Li, H. P.; Bazan, G. C. Conjugated Oligoelectrolyte/SS-DNA Aggregates: Self-Assembled Multicomponent Chromophores for Protein Discrimination. *Adv. Mater.* **2009**, *21*, 964−967.

(25) Schwille, P.; Kummer, S.; Heikal, A. A.; Moerner, W. E.; Webb, W. W. Fluorescence Correlation Spectroscopy Reveals Fast Optical Excitation-Driven Intramolecular Dynamics of Yellow Fluorescent Proteins. *Proc. Natl. Acad. Sci. U.S.A.* **2000**, *97*, 151−156.

(26) Pack, C. G.; Nishimura, G.; Tamura, M.; Aoki, K.; Taguchi, H.; Yoshida, M.; Kinjo, M. Analysis of Interaction between Chaperonin Groel and Its Substrate Using Fluorescence Correlation Spectroscopy. *Cytometry* **1999**, *36*, 247−253.

(27) Borsch, M.; Turina, P.; Eggeling, C.; Fries, J. R.; Seidel, C. A. M.; Labahn, A.; Graber, P. Conformational Changes of the H⁺-Atpase from *Escherichia coli* upon Nucleotide Binding Detected by Single Molecule Fluorescence. *FEBS Lett.* **1998**, *437*, 251−254.

(28) Xu, Z. H.; Tsai, H. H.; Wang, H. L.; Cotlet, M. Solvent Polarity Effect on Chain Conformation, Film Morphology, and Optical Properties of a Water-Soluble Conjugated Polymer. *J. Phys. Chem. B* **2010**, *114*, 11746−11752.

(29) Medina, M. A.; Schwille, P. Fluorescence Correlation Spectroscopy for the Detection and Study of Single Molecules in Biology. *Bioessays* **2002**, *24*, 758−764.

(30) Elson, E. L.; Magde, D. Fluorescence Correlation Spectroscopy 0.1. Conceptual Basis and Theory. *Biopolymers* **1974**, *13*, 1−27.

(31) Aragon, S. R.; Pecora, R. Fluorescence Correlation Spectroscopy as a Probe of Molecular Dynamics. *J. Chem. Phys.* **1976**, *64*, 1791−1803.

(32) Wu, D. L.; Feng, F. D.; Xie, D. P.; Chen, Y.; Tan, W. H.; Schanze, K. S. Helical Conjugated Polyelectrolyte Aggregation Induced by Biotin−Avidin Interaction. *J. Phys. Chem. Lett.* **2012**, *3*, 1711−1715.

(33) Paolesse, R.; Monti, D.; Dini, F.; Di Natale, C. In *Luminescence Applied in Sensor Science*; Springer-Verlag Berlin: Berlin, Heidelberg, 2011; Vol. *300*, pp 139−174.

(34) Demchenko, A. P. The Future of Fluorescence Sensor Arrays. *Trends Biotechnol.* **2005**, *23*, 456−460.

(35) Bajaj, A.; Miranda, O. R.; Phillips, R.; Kim, I. B.; Jerry, D. J.; Bunz, U. H. F.; Rotello, V. M. Array-Based Sensing of Normal, Cancerous, and Metastatic Cells Using Conjugated Fluorescent Polymers. *J. Am. Chem. Soc.* **2010**, *132*, 1018−1022.

(36) Selkoe, D. J. Folding Proteins in Fatal Ways. *Nature* **2003**, *426*, 900−904.

(37) Aebersold, R.; Mann, M. Mass Spectrometry-Based Proteomics. *Nature* **2003**, *422*, 198−207.

(38) Johnson, C. J.; Zhukovsky, N.; Cass, A. E. G.; Nagy, J. M. Proteomics, Nanotechnology and Molecular Diagnostics. *Proteomics* **2008**, *8*, 715−730.

(39) Fields, S. Proteomics: Proteomics in Genomeland. *Science* **2001**, *291*, 1221−1224.

(40) Yang, J.; Wu, D.; Xie, D.; Feng, F.; Schanze, K. S. Ion-Induced Aggregation of Conjugated Polyelectrolytes Studied by Fluorescence Correlation Spectroscopy. *J. Phys. Chem. B* **2013**, *117*, 16314−16324.

(41) Total Protein Assays, http://www.science.smith.edu/departments/Biochem/Biochem_353/Bradford.html, 2012, (accessed April 18, 2014), maintained by Smith College, Department of Biochemistry.

(42) Chen, Y. Analysis and Applications of Fluorescence Fluctuation Spectroscopy. Ph. D. Dissertation, University of Illinois at Urbana-Champaign, 1999.

(43) Magde, D.; Elson, E. L.; Webb, W. W. Fluorescence Correlation Spectroscopy 0.2. Experimental Realization. *Biopolymers* **1974**, *13*, 29−61.

(44) Rigler, R.; Mets, U.; Widengren, J.; Kask, P. Fluorescence Correlation Spectroscopy with High Count Rate and Low-Background: Analysis of Translational Diffusion. *Eur. Biophys. J.* **1993**, *22*, 169−175.

(45) Aragon, S. R.; Pecora, R. Fluorescence Correlation Spectroscopy and Brownian Rotational Diffusion. *Biopolymers* **1975**, *14*, 119−137.

(46) Prince, R. B.; Saven, J. G.; Wolynes, P. G.; Moore, J. S. Cooperative Conformational Transitions in Phenylene Ethynylene Oligomers: Chain-Length Dependence. *J. Am. Chem. Soc.* **1999**, *121*, 3114−3121.

(47) As shown in the webpage of Sigma company, HK3 has two isoforms, PI and PII (A and B), pI = 5.25 and 4, respectively.

(48) HRP has at least seven isozymes with pI values range from 3.0 to 9.0 as described in the webpage of the Sigma-Aldrich company.

(49) Bradford, M. M. Rapid and Sensitive Method for Quantitation of Microgram Quantities of Protein Utilizing Principle of Protein-Dye Binding. *Anal. Biochem.* **1976**, *72*, 248−254.

(50) Schwille, P.; Ries, J. In *Biophotonics: Spectroscopy, Imaging, Sensing, and Manipulation*; Di Bartolo, B., Collins, J. M., Eds.; Springer: Dordrecht, The Netherlands, 2011; p 76−77.

(51) Berglund, A. J.; Mabuchi, H. Tracking-Fcs: Fluorescence Correlation Spectroscopy of Individual Particles. *Opt. Express* **2005**, *13*, 8069−8082.

(52) Wang, Y.; Chi, E. Y.; Schanze, K. S.; Whitten, D. G. Membrane Activity of Antimicrobial Phenylene Ethynylene Based Polymers and Oligomers. *Soft Matter* **2012**, *8*, 8547−8558.

(53) Johnson, R. A.; Wichern, D. W. *Applied Multivariate Statistical Analysis*, 2nd ed.; Prentice-Hall: Englewood Cliffs, NJ, 1988.

(54) Jurs, P. C.; Bakken, G. A.; McClelland, H. E. Computational Methods for the Analysis of Chemical Sensor Array Data from Volatile Analytes. *Chem. Rev.* **2000**, *100*, 2649−2678.

(55) Loog, M.; Duin, R. P. W.; Haeb-Umbach, R. Multiclass Linear Dimension Reduction by Weighted Pairwise Fisher Criteria. *IEEE T. Pattern Anal.* **2001**, *23*, 762−766.

(56) Uray, M.; Roth, P. M.; Bischof, H. Efficient Classification for Large-Scale Problems by Multiple Lda Subspaces. *Proc. Int. Conf. on Computer Vision Theory and Applications—VISAPP 1*; 2009, pp 299−306. Available online: http://dblp.uni-trier.de/db/conf/visapp/visapp2009-1.html#UrayRB09.